ORGANIC LETTERS

2012
Vol. 14, No. 12
3076–3079

Band Gap of Carbon–Sulfur [*n*]Helicenes

Makoto Miyasaka,[†] Maren Pink,[‡] Arnon Olankitwanit,[†] Suchada Rajca,[†] and Andrzej Rajca*[,†]

Department of Chemistry, University of Nebraska, Lincoln, Nebraska 68588-0304, United States, and IUMSC, Department of Chemistry, Indiana University, Bloomington, Indiana 47405-7102, United States

arajca1@unl.edu

Received April 27, 2012

ABSTRACT

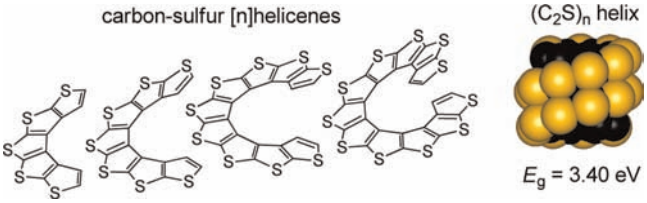

Asymmetric synthesis of (−)-[9]helicene, as well as preparation of its lower homologues, completes the series of carbon–sulfur [5]-, [7]-, [9]-, and [11]helicenes. Spectroscopic and electrochemical studies of this series provide an absorption onset-based band gap, E_g = 3.40 eV, for a cross-conjugated $(C_2S)_n$ helix; this value may be compared to E_g = 3.59 eV obtained from TD-DFT computed excitation energies for a series of dimethyl-substituted [*n*]helicenes ($n \leq 31$).

[*n*]Helicenes are molecules with π-systems consisting of *ortho*-fused aromatic rings adopting a helical shape.[1−5] For larger *n*, the helicity and ladder connectivity of the π-system lead to significant barriers for racemization and strong chiral properties.[2,4] Despite recent advances in the synthesis of [*n*]helicenes and [*n*]helicene-like molecules,[5−8] asymmetric synthesis of long [*n*]helicenes, $n \geq 9$, remains challenging.[8,9]

To date, there is only one report of the asymmetric synthesis of carbon–sulfur [11]helicene in which 11 thiophene rings are fused into a helical π-system, fragments of a $(C_2S)_n$ helix (Figure 1).[9] Such helical oligothiophenes[10,11] are of interest as building blocks for chiral materials.[3−5,12,13] These structures provided the first configurationally stable [*n*]helicene radical cation[14] and are characterized by strong, [*n*]helicene-like chirooptical properties, despite a low degree of electron delocalization in their cross-conjugated π-systems.[15]

Insight into the electronic structure of [*n*]helicenes is important to the design of materials with strong chiral properties.[4,14] Systematic experimental studies of their

[†] University of Nebraska.
[‡] Indiana University.

(1) Newman, M. S.; Lednicer, D. *J. Am. Chem. Soc.* **1956**, *78*, 4765–4770.
(2) Martin, R. H. *Angew. Chem., Int. Ed. Engl.* **1974**, *13*, 649–659.
(3) Rajca, A.; Rajca, S.; Pink, M.; Miyasaka, M. *Synlett* **2007**, 1799–1822.
(4) Rajca, A.; Miyasaka, M. In *Functional Organic Materials - Syntheses and Strategies*; Mueller, T. J. J., Bunz, U. H. F., Eds.; Wiley-VCH: New York, 2007; pp 543−577.
(5) Shen, Y.; Chen, C.-F. *Chem. Rev.* **2012**, *112*, 1463–1535.
(6) (a) Nakano, K.; Oyama, H.; Nishimura, Y.; Nakasako, S.; Nozaki, K. *Angew. Chem., Int. Ed.* **2012**, *51*, 695–699. (b) Sawada, Y.; Furumi, S.; Takai, A.; Takeuchi, M.; Noguchi, K.; Tanaka, K. *J. Am. Chem. Soc.* **2012**, *134*, 4080–4083.
(7) Jierry, L.; Harthong, S.; Aronica, C.; Mulatier, J.-C.; Guy, L.; Guy, S. *Org. Lett.* **2012**, *14*, 288–291.
(8) Sehnal, P.; Stará, I. G.; Saman, D.; Tichý, M.; Míšek, J.; Cvačka, J.; Rulíšek, L.; Chocholoušová, J.; Vacek, J.; Goryl, G.; Szymonski, M.; Císařová, I.; Starý, I. *Proc. Natl. Acad. Sci. U.S.A.* **2009**, *106*, 13169–13174.
(9) Miyasaka, M.; Rajca, A.; Pink, M.; Rajca, S. *J. Am. Chem. Soc.* **2005**, *127*, 13806–13807.
(10) Mishra, A.; Ma, C.-Q.; Bäuerle, P. *Chem. Rev.* **2009**, *109*, 1141–1276.
(11) (a) Rajca, A.; Wang, H.; Pink, M.; Rajca, S. *Angew. Chem., Int. Ed.* **2000**, *39*, 4481–4483. (b) Rajca, A.; Miyasaka, M.; Pink, M.; Wang, H.; Rajca, S. *J. Am. Chem. Soc.* **2004**, *126*, 15211–1522. (c) Miyasaka, M.; Pink, M.; Rajca, S.; Rajca, A. *Angew. Chem., Int. Ed.* **2009**, *48*, 5954–5957.
(12) Miyasaka, M.; Rajca, A.; Pink, M.; Rajca, S. *Chem.—Eur. J.* **2004**, *10*, 6531–6539.
(13) (a) Miyasaka, M.; Pink, M.; Rajca, S.; Rajca, A. *Org. Lett.* **2010**, *12*, 3230–3233. (b) Swager, T. M.; Batson, J. *Synfacts* **2010**, 1136–1136.
(14) Zak, J. K.; Miyasaka, M.; Rajca, S.; Lapkowski, M.; Rajca, A. *J. Am. Chem. Soc.* **2010**, *132*, 3246–3247.
(15) Rajca, A.; Miyasaka, M.; Pink, M.; Xiao, S.; Rajca, S.; Das, K.; Plessel, K. *J. Org. Chem.* **2009**, *74*, 7504–7513.
(16) (a) Han, S.; Bond, A. D.; Disch, R. L.; Holmes, D.; Schulman, J. M.; Teat, S. J.; Vollhardt, K. P. C.; Whitener, G. D. *Angew. Chem., Int. Ed.* **2002**, *41*, 3223–3227. (b) Han, S.; Anderson, D. R.; Bond, A. D.; Chu, H. V.; Disch, R. L.; Holmes, D.; Schulman, J. M.; Teat, S. J.; Vollhardt, K. P. C.; Whitener, G. D. *Angew. Chem., Int. Ed.* **2002**, *41*, 3227–3230.

10.1021/ol3011437
Published on Web 05/31/2012

electronic properties, including extrapolations of band gaps from electronic absorption onsets and/or electrochemical onset potentials, are lacking because of the scarcity of homologous [*n*]helicenes.[9,16−18] Computational studies of band gaps are limited to density functional theory (DFT) extrapolation of the gas phase HOMO−LUMO gaps.[19]

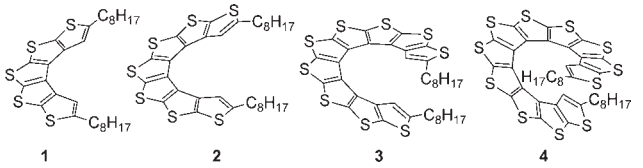

Figure 1. Carbon−sulfur [*n*]helicenes, $n = 5, 7, 9, 11$.

Herein we report the asymmetric synthesis of (−)-[9]helicene and determination of the band gap of a cross-conjugated $(C_2S)_n$ helix. Homologues of the carbon−sulfur [5]-, [7]-, [9]-, and [11]helicenes (Figure 1), with solubilizing *n*-octyl chains, are prepared to provide electronic spectroscopic (UV−vis absorption and circular dichroism) and electrochemical data for band gap determination, which are then compared to the results obtained from DFT and time-dependent DFT (TD-DFT) computations.

Syntheses of carbon−sulfur [*n*]helicenes rely on iterative sequences of connection and annelation steps: CC bond formation between two sterically hindered and less reactive *β*-positions of thiophenes, and mono- or diannelation, forming two or four CS bonds that make up one or two thiophene rings in a nonplanar geometry.

Scheme 1. Synthesis of [5]Helicene **1** and [7]Helicene **2**[a]

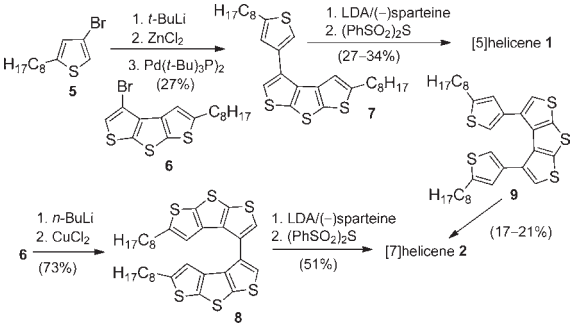

[a] Isolated yields; **7** partially purified.

In the synthesis of [5]helicene **1** and [7]helicene **2** (Scheme 1), the CC bond forming steps are implemented by Negishi cross-coupling.[20] The organozinc derived from 4-bromo-2-octylthiophene (**5**)[20] reacts with 4-bromo-5′-octyldithieno-[2,3-*b*:3′,2′-*d*]thiophene (**6**)[21] to give tetrathiophene **7**, while Cu(II)-mediated oxidation of the organolithium[11,22,23] derived from **6** gives hexathiophene **8**. Monoannelation steps are implemented by LDA/(−)-sparteine-mediated deprotonation of the two α-positions of the thiophene moieties in **7** and **8** to provide the corresponding carbodianion. Subsequent addition of an electrophilic source of sulfur, $(PhSO_2)_2S$, leads to ring annelation, forming [5]helicene **1** and [7]helicene **2**, respectively. Alternatively, [7]helicene **2** can be prepared in moderate yield by diannelation of pentathiophene **9**,[20] using similar reaction conditions to monoannelation.

In the synthesis of [9]helicene **3** (Scheme 2), the CC bond forming step relies on the Pd-mediated homocoupling[9] between **6**[21] and bromotetrathiophene **10**[20] (1:1 molar ratio), to provide heptathiophene **11** in about 50% yield. In addition, this reaction gives oligothiophenes **8** and **12**, precursors to [7]helicene **2** and [11]helicene **4**,[9] in about 20% yields. Diannelation of **11**, using LDA/(−)-sparteine and $(PhSO_2)_2S$, produces [9]helicene **3** in 15% yield and an enantiomeric excess (ee) of 14%.

The structure of **3** is confirmed by single-crystal synchrotron X-ray analysis (Figure 2). The oligothiophene has an approximate C_2 point group of symmetry.

Scheme 2. Asymmetric Synthesis of [9]Helicene **3**[a]

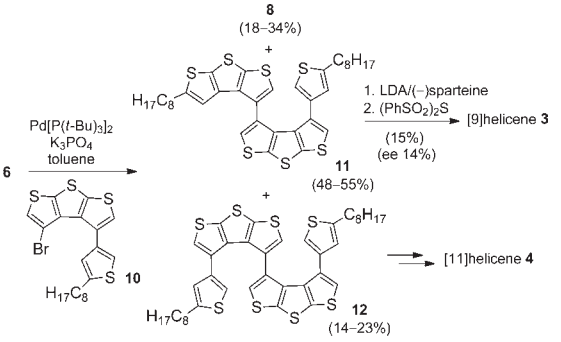

[a] Isolated yields.

UV−vis spectra of 5,5′-dioctyldithieno[2,3-*b*:3′,2′-*d*]-thiophene (trithiophene **13**)[21] and [*n*]helicenes **1**−**4** show a progressive red shift with the increasing number of thiophene rings, though the values of λ_{max} for **13** and **1** are outliers in this trend. A similar red shift is observed for the longest wavelength bands in the CD spectra of **3** and **4** (Figure 3). Absorption onsets, λ_{onset}, determined by the standard tangent method (Supporting Information (SI)), provide a more

(17) Bossia, A.; Falciola, L.; Graiff, C.; Maioranaa, S.; Rigamontia, C.; Tiripicchioc, A.; Licandroa, E.; Mussini, P. R. *Electrochim. Acta* **2009**, *54*, 5083–5097.

(18) E_g = 2.5, 2.4, and 2.1 eV was estimated for [*n*]helicenes, [*n*]thiahelicenes, and [*n*]heliphenes, respectively, via extrapolation of λ_{max} (refs 4 and 16).

(19) Tian, Y.-H.; Park, G.; Kertesz, M. *Chem. Mater.* **2008**, *20*, 3266–3277.

(20) Miyasaka, M.; Rajca, A. *Synlett* **2004**, 177–181.

(21) Miyasaka, M.; Rajca, A. *J. Org. Chem.* **2006**, *71*, 3264–3266.

(22) Wittig, G.; Klar, G. *Liebigs Ann. Chem.* **1967**, *704*, 91–108.

(23) (a) Rajca, A.; Safronov, A.; Rajca, S.; Wongsriratanakul, J. *J. Am. Chem. Soc.* **2000**, *122*, 3351–3357. (b) Rajca, A.; Wang, H.; Bolshov, P.; Rajca, S. *Tetrahedron* **2001**, *57*, 3725–3735. (c) Rajca, A.; Rajca, S. *Angew. Chem., Int. Ed.* **2010**, *49*, 672–674.

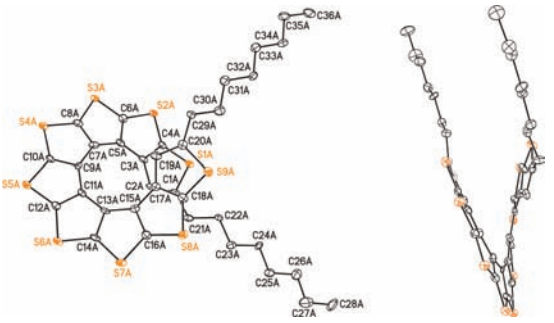

Figure 2. Synchrotron X-ray structure for [9]helicene **3**. Carbon and sulfur atoms are depicted with thermal ellipsoids set at the 50% probability level. Hydrogens atoms are omitted.

reliable measure of the observed red shift and, thus, the band gap, E_g. The plot of UV−vis λ_{onset} versus $1/N_\pi$, where N_π is the number of electrons in the π-system of **1**−**4**, provides $E_g = 3.40$ eV for the $(C_2S)_n$ helix. A similar plot of CD λ_{onset}, using only two available data points (**3** and **4**), gives $E_g = 3.61$ eV (Figure 5).

Chirooptical data for **3** such as a negative specific rotation, $[\alpha]_D^{rt} < 0$, and negative longest wavelength CD band, $\Delta\varepsilon_{max} < 0$) (Figure 3), suggest that the obtained excess of (−)-**3** corresponds to the (*M*)-enantiomer. This (−)-sparteine-mediated stereoselection of (*M*)-[9]helicene **3** is consistent with the analogous monoannelations producing (*M*)-[11]helicene **4** and related helicenes,[9,11] as well as (*R*)-biaryl-based tetraarylenes,[23] and it is opposite to that in the triannelation of **12** to provide (*P*)-**4**.[9]

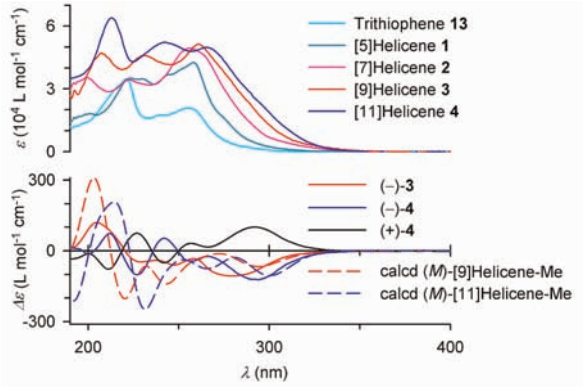

Figure 3. Electronic spectra of [*n*]helicenes: UV−vis absorption and CD in cyclohexane; TD-DFT calculated CD spectra for dimethyl-substituted [9]- and [11]helicene using the B3LYP/6-31G(d) and the IEF-PCM-UFF model for cyclohexane.

[*n*]Helicenes **1**−**4** are examined by cyclic voltammetry (CV) and square wave voltammetry (SWV) in dichloromethane (CH_2Cl_2) and tetrahydrofuran (THF). CV in CH_2Cl_2 indicates reversible oxidations and irreversible reductions (Figure 4).[24] The oxidation to radical cations becomes more facile with the increasing length of the [*n*]helicene from $n = 5, 7, 9$, to 11, as indicated by the decreasing first oxidation potentials $E^{1+/0}$ (and onset potentials, E_{onset}^{ox}) (Table 1). SWV provides second oxidation potentials, $E^{2+/+}$, which decrease steeply with increasing n. Notably, $E^{3+/2+}$ and $E^{4+/3+}$ for **4**, with $n = 11$, could be determined as well.

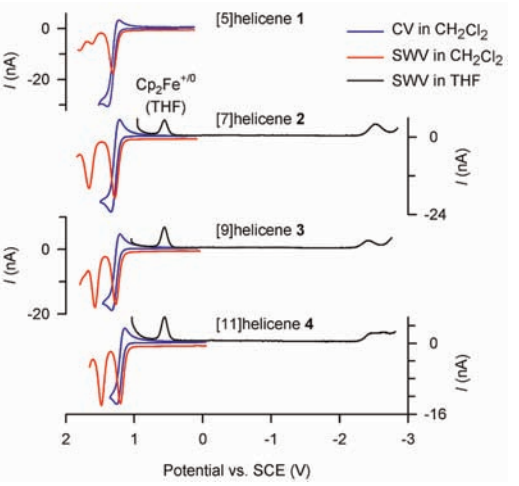

Figure 4. Cyclic voltammetry (CV) and square wave voltammetry (SWV) for [*n*]helicenes.

Although the CV of **2**−**4** in THF is not reversible, reduction potentials, $E^{-/0}$, (and onset potentials, E_{onset}^{red}) could be approximately determined by SWV. However, the SWV reduction peaks are relatively broad (Figure 4), possibly due to the instability of the corresponding radical anion, which could make the observed $E^{-/0} \approx -2.5$ V (and E_{onset}^{red}) less negative (Table 1).

The differences between SWV onset potentials for oxidation and reduction, $\Delta E_{onset} = E_{onset}^{ox} - E_{onset}^{red}$, for [*n*]helicenes, $n = 7, 9$, and 11, are plotted versus $1/N_\pi$ to provide a straight line which extrapolates to $E_g = 3.16$ eV (Figure 5).

The geometries of the simplified structures of carbon−sulfur [*n*]helicenes in which the octyl chains are replaced with methyl groups, [*n*]helicenes-Me, with $n = 5, 7, 9, ..., 31$ were optimized at the B3LYP/6-31G(d)/IEF-PCM-UFF and B3LYP/6-31G(d,p)/IEF-PCM-UFF levels of theory, using the solvent model for cyclohexane and constraining molecular symmetry to a C_2 point group of symmetry.[26] Electronic UV−vis and CD spectra for [*n*]helicenes-Me with *n* up to 15 were computed using the TD-DFT approach at the B3LYP/6-31G(d)/IEF-PCM-UFF level (Figure S53, SI). For [*n*]helicenes-Me with $n = 9$ and 11, a red shift for the calculated Gaussian envelopes of longest wavelength bands is observed, compared to the experimental spectra for **3** and **4** (Figure 3).[15]

(24) CV of **1** is only reversible at higher potential scanning rates.

(25) Connelly, N. G.; Geiger, W. E. *Chem. Rev.* **1996**, *96*, 877–910.
(26) Frisch, M. J. et al. *Gaussian 09*, revision A.01; Gaussian: Wallingford, CT, 2009.

Table 1. Electrochemical Oxidation (CH_2Cl_2) and Reduction (THF) of [*n*]Helicenes[a]

	oxidation					E_g (V)		reduction		
		CV (V)		SWV (V)				SWV (V)		
	E	$E_{1/2}^{ox}$	E_{onset}^{ox}	E_p^{ox}	E_{onset}^{ox}	ΔE_p	ΔE_{onset}	E_p^{red}	E_{onset}^{red}	E
1	$E^{+/0}$	1.308 ± 0.004	1.23	1.312 ± 0.004	1.22	-	-	-	-	-
	$E^{2+/+}$			1.81						
2	$E^{+/0}$	1.277 ± 0.002	1.21	1.282 ± 0.006	1.18	3.83	3.53	−2.546 ± 0.048	−2.35	$E^{-/0}$
	$E^{2+/+}$			1.661 ± 0.008						
3	$E^{+/0}$	1.266 ± 0.004	1.20	1.271 ± 0.004	1.19	3.70	3.45	−2.431 ± 0.038	−2.26	$E^{-/0}$
	$E^{2+/+}$	1.56		1.574 ± 0.004						
	$E^{3+/2+}$			2.009						
4	$E^{+/0}$	1.196 ± 0.004	1.12	1.200 ± 0.004	1.10	3.69	3.40	−2.488 ± 0.018	−2.30	$E^{-/0}$
	$E^{2+/+}$	1.47		1.478 ± 0.002				−2.633 ± 0.022		$E^{2-/-}$
	$E^{3+/2+}$			1.802 ± 0.014						
	$E^{4+/3+}$			1.99 ± 0.11						

[a] Potentials (vs SCE) from multiple voltammograms with scan rates of 50−500 mV s^{-1} or with a frequency of 10 Hz. Supporting electrolyte: 0.1 M $[n\text{-}Bu_4N]^+[PF_6]^-$. Ferrocene as internal standard: $Cp_2Fe^{+/0}$ at +0.460 and +0.560 V in CH_2Cl_2 and THF, respectively.[25] For determination of onset potentials, see Figures S24−S52, SI.

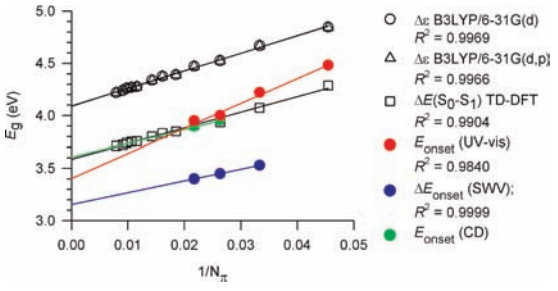

Figure 5. Extrapolated E_g for $(C_2S)_n$ helix using theory ($\Delta\varepsilon$ and $\Delta E(S_0-S_1)$) and experiment (UV−vis, SWV, and CD).

The DFT-computed HOMO−LUMO energy gaps ($\Delta\varepsilon$) and the TD-DFT-computed vertical excitation energies to the lowest excited state ($\Delta E(S_0-S_1)$) are plotted versus $1/N_\pi$ (Figure 5). Extrapolation of the $\Delta\varepsilon$ plot provides E_g = 4.09 eV,[27] which significantly overestimates the experimental E_g determined from the UV−vis λ_{onset} (3.40 eV) and electrochemical ΔE_{onset} (3.16 eV) (Figure 5). However, this extrapolated E_g is in better agreement with the E_g = 4.38 eV derived from λ_{max} for **2**, **3**, and **4**.

Extrapolation of the ($\Delta E(S_0-S_1)$) plot[28] provides E_g = 3.59 eV, which is in better agreement with E_g = 3.40 eV, obtained from λ_{onset} for **1**, **2**, **3**, and **4** (Figure 5). When only the two longest available [*n*]helicenes, **3** and **4**, are considered, extrapolation of the experimental UV−vis and CD λ_{onset} provide E_g = 3.71 and 3.61 eV, respectively.

B3LYP/6-31+G(d,p)/IEF-PCM-UFF studies of [*n*]helicene-Me, n = 7 and 9, suggest that C_2-symmetric helical radical cations are stable, but for similar radical anions, geometry reoptimization leads to an energy drop of 0.7−0.8 eV, to produce minima in which one of the C−S bonds is broken (Figure S54, SI). This might be the origin for the relatively low value of the electrochemical E_g = 3.16 eV.

In conclusion, the band gap of a cross-conjugated $(C_2S)_n$ helix is best estimated using absorption onsets, with TD-DFT-calculated excitation energies $\Delta E(S_0-S_1)$ providing the closest agreement between the experiment and theory. Synthesis of longer carbon−sulfur [*n*]helicenes, $n > 11$, would allow for testing whether the agreement between the experiment and theory would further improve.

Acknowledgment. We thank the National Science Foundation for support of this work through Grants CHE-0718117 and CHE-1012578.

Supporting Information Available. Complete acknowledgment and ref 26, experimental and computational details. This material is available free of charge via the Internet at http://pubs.acs.org.

(27) Kertesz reported similar value, E_g = 4.10 eV, based upon extrapolation of $\Delta\varepsilon$ for unsubstituted carbon−sulfur [*n*]helicenes, $n \leq 30$, at the B3LYP/6-31(d) in the gas phase: Reference 19.

(28) (a) Risko, C.; McGehee, M. D.; Bredas, J. L. *Chem. Sci.* **2011**, *2*, 1200–1218. (b) Rajca, A.; Boratynski, P. J.; Olankitwanit, A.; Shiraishi, K.; Pink, M.; Rajca, S. *J. Org. Chem.* **2012**, *77*, 2107–2120.

The authors declare no competing financial interest.